

# EXPERIMENTAL STUDY ON R1234YF HEAT PUMP AT LOW AMBIENT TEMPERATURE AND COMPARISON WITH OTHER REFRIGERANTS

*Shuxue Xu<sup>1</sup>, Jianhui Niu<sup>2</sup>, Guoyuan Ma<sup>\*1</sup>,*

<sup>1</sup> College of Environmental and Energy Engineering, Beijing University of Technology, Beijing 100124, China

<sup>2</sup> College of Energy and Environmental Engineering, Hebei University of Architecture, Zhangjiakou 075000, China

\* Guoyuan Ma; E-mail: xsx@bjut.edu.cn

*In this paper, an integrated vapor injection compression heat pump system using R1234yf and R32, R410A, R22 and R134a as working fluids was developed, and their heating performances under low ambient temperature were quantitatively evaluated. An experimental bench was built to test the system's working performance. The condensing temperature, evaporating temperature, power input, and other variables were analyzed to evaluate the system's heating capability and energy efficiency. Test results showed that the R1234yf system can run at the evaporating temperature of -20 °C, but its heating Coefficient of Performance (COP) was 5% lower than R134a; The R1234yf vapor injection system provided very significant performance improvements for heating performance compared with no vapor injection: the heating capacity and heating COP can be improved by 14.3% and 11.7%, respectively.*

**Key words:** R1234yf, Vapor injection, Heat pump, Refrigeration

## 1. Introduction

Many refrigeration working fluids can be used in vapor compression domestic air conditioner systems, including Hydrochlorofluorocarbons (HCFCs, such as R22), Hydrofluorocarbons (HFCs, such as R410A and R32) and natural alternatives such as propane (R290), isobutene (R600a), and carbon dioxide (R744). R744 is not a feasible alternative because its pressure is too high [1]. R290 and R600a are strong candidates and have many benefits: they are cheap, non-toxic, chemically stable, compatible with many materials, and miscible with mineral oils. While their drawback is their flammability[2]. R22 and R410A are widely used in vapor compression refrigeration and air conditioning systems due to their high energy efficiency ratio [3]. Recently, R32 has also been considered as an important alternative for use in small to medium capacity air conditioners and heat pumps by many countries. Besides the influence of the environmental consideration (Ozone Depletion Potential, ODP and Global Warming Potential, GWP), Which fluid adopted in an air conditioner will depend on the operating conditions, for example, in a domestic air conditioner at low ambient temperature, the temperature of the environment (the heat sink) starts at -20°C and ends at far above 35°C [4]. Running under the above condition, all of the working fluids have the same problems: the discharge temperature is too high, and the heating capacity decrease seriously. Experiment results

have shown that the discharge temperature of both R22 and R410A are higher than 120 °C when running under the condition of lower than -15 °C. The discharge temperature of the R32 compressor is typically approximately 12 °C higher than that of R410A in standard air conditioning conditions, and the excess may be over 30 °C in severe conditions, such as with an ambient temperature lower than -15 °C [5]. The extremely high discharge temperature reduces the reliability of system's operation due to the possibility of lubricating oil degradation, and leads to the limited operating envelope of compressors.

R1234yf, which has zero ODP and a GWP value of 4 only, has been introduced as a suitable replacement for HFC in a variety of refrigeration and air conditioning applications. Mota-Babiloni et al. [6] compared the cooling capacity and the coefficient of performance (COP) values of R1234yf and R1234ze (E), and the results showed that the cooling capacity and COP values of both alternative refrigerants were found to be about 9 to 30% and 6% lower than R134a. Bolaji et al. [7] theoretically investigated refrigerants with low GWP as substitutes for R134a, and the results showed that the cooling capacity of R1234yf was smaller than that of R134a for different evaporation temperatures. Zilio et al. [8] directly used R1234yf as an alternative to R134a, and changed the expansion valve adjustments. The results were presented for different compressor speeds and ambient temperatures. Navarro-Esbri et al. [9] performed an experimental investigation on the direct use of R1234yf in a system operating with R134a. They stated that a reduction in the cooling capacity of 6% to 13% approximately was noted using R1234yf instead of R134a. Xu et al. [10] developed an integrated gas-injected scroll compressor heat pump system using R1234yf, R32 and its binary mixtures as a working fluid, and the results showed that a R1234yf/R32 mixture can run at an evaporating temperature of -20 °C, and it has the highest heating COP value between R1234yf and R32.

Various technologies have been found to be conducive to decreasing discharge temperature. These concepts include two-stage compression systems with inter-cooling, or in a cascade arrangement, systems which inject two-phase refrigerant into the compressor, and systems which use cooled lubrication oil to cool the compressor. Among all the above methods, a vapor injection system with the advantages of a simple structure and consistency with the basic principles of thermodynamics is considered to be promising for wide application. In this situation, the discharge temperature would be sharply decreased [11]. Dutta et al. [12] theoretically and experimentally investigated the influence of liquid refrigerant on the performance of an R22 high-side scroll compressor, and found that the oil temperature decreased with increasing injection ratio and lead to a slight improvement in performance. Winandy et al. [13] studied the effects of liquid injection on the discharge temperature of an R22 compressor, and their results showed that the discharge temperature decreased linearly with injection ratio. For each percentage of liquid injection, discharge temperature decreased by approximately 1.2 °C. Cho et al. [14] studied the influence of liquid injection on an inverter-driven low-side scroll compressor at different compressor frequencies. It was concluded that liquid injection under high frequency was very effective at attaining higher performance and reliability of the compressor, whereas injection under low frequency showed some disadvantages with respect to compressor power, capacity, and adiabatic efficiency due to high leakage through the gap in the scroll wrap. Gas refrigerant injection is an important technique to improve the cooling capacity and COP [15]. Zhang et al. [16] built an R134a heat pump system with vapor injection, results found that under -20 °C ambient temperature, an average improvement of 57.7% in heating capacity can be achieved. A number of studies on gas injection have also proven that gas injection provides significant enhancement in capacity and COP

[17-20]. In addition, gas injection demonstrates a decrease in discharge temperature, though the cooling effect provided by the vapor refrigerant is limited [21].

In this study, a composite test system consisting of second-refrigerant calorimeter and water-cooled condenser was built. The performances of an R1234yf heat pump at low ambient temperature were measured, and its heating performance was also compared with R32, R410A, R22 and R134a. The effect of the vapor suction superheat on the heating performance of a single-stage system was experimentally researched; the vapor injection system was also established and its heating characteristics were compared with the single-stage system at various operating conditions.

## 2. Experimental Setup and Procedure

### 2.1. Vapor Injection Heat Pump System (VI system)

The operating fundamentals of the vapor injection compression heat pump system are shown in Fig.1.

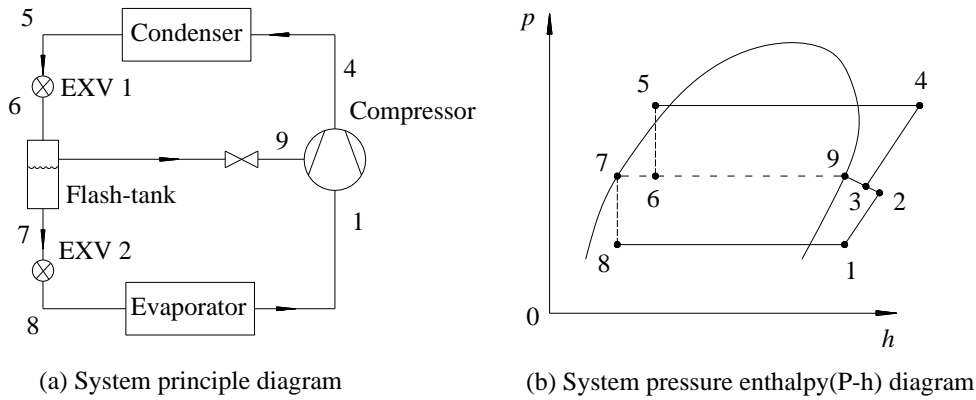


**Fig. 1. Heat pump with vapor injection (VI system)**

Fig.1. we can see that the system has a flash-tank with the system compressor having supplementary inlets. The high pressure refrigerant from the condenser flows into expansion valve 1 (EXV1), and its pressure drops to intermediate pressure, and then enters into the flash-tank. In the flash-tank, the refrigerant is separated into pure liquid and saturated vapor. On one hand, the liquid refrigerant from the bottom of the flash-tank flows into expansion valve 2 (EXV2), and its pressure drops to the evaporating pressure, and then enters into the evaporator; on the other hand, the saturated vapor leaving from the top of the flash-tank is injected into the compressor with suitable pressure.

To ensure that the heating performance of the system is relatively high under the condition of low temperature, there are two key parameters for the system: the optimal location of the vapor injection inlets and the most suitable vapor injection pressure, both the two parameters were derived from experiment and calculation suggested by Xu et al. [18]. Equation (1) was used to calculate the most suitable vapor injection pressure.

$$p_m = k\sqrt{p_e p_c} \quad (1)$$

Where,  $p_e$  is evaporating pressure [MPa],  $p_c$  is condensing pressure [MPa],  $k$  is factor of vapour injection pressure.

As shown in Fig.2. the heating  $COP$  almost increase firstly and then decrease with the increasing of the relative vapour injection pressure factor,  $k$ . At a certain value of  $k$ , heating  $COP$  reaches the maximum value, respectively. For example,  $k$  is 1.2 when heating  $COP$  is the biggest

under the condition of  $t_o=0^\circ\text{C}$ . The favourable value of  $k$  should be between 1.15 and 1.35 when the evaporating temperature is  $-10$ - $0^\circ\text{C}$ . These results are fundamental for adjusting the R1234yf system with vapour injection.

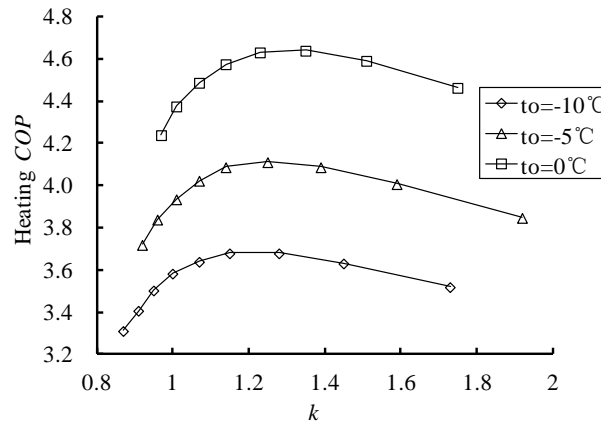


Fig. 2. The variation of heating COP with  $k$

## 2.2. Experimental Apparatus and Procedure

The experimental tests are carried out in a fully monitored vapor compression plant; a schematic diagram for the plant is shown in Fig.3.

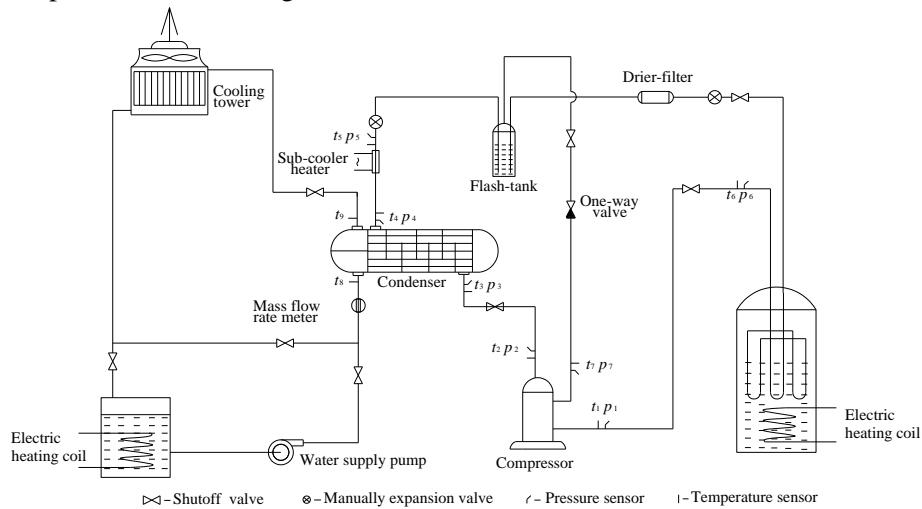


Fig. 3. Schematic diagram of experimental heat pump

As shown in Fig.3. we can see that the system has a second-refrigerant calorimeter and a water-cooled condenser. A scroll compressor originally designed with two manually controlled expansion valves used to regulate the mass flow rate and vapor injection pressure. The evaporating temperature (pressure) is adjusted by the manual expansion valves, and the vapor suction temperature is adjusted by the electric power input of the second-refrigerant calorimeter, the calorimeter use R123 as the second-refrigerant and it also contains an electric heaters coil located downstream of the calorimeter, the electric heaters can be controlled between 0-12kW respectively, to provide the required vapor suction temperatures at the inlets of the compressor. The heating capacity is the enthalpy difference multiplied by the mass flow rate of the liquid refrigerant through them, respectively. The temperatures and pressures of the fluids at the inlet and outlet of the condenser or evaporator were measured by the sensors or transducers, and the enthalpy can be obtained from the measured data. Fig.4. shows a photograph of the experimental system.



Fig. 4. Photo of the actual breadboard system

$$q_{mf} = \frac{cm(t_9 - t_8)}{h_3 - h_4} \quad (2)$$

Where,  $q_{mf}$  is mass flow rate of liquid refrigerant throw condenser( $\text{kgs}^{-1}$ ),  $m$  is water flow rate throw condenser( $\text{kgs}^{-1}$ ),  $c$  is the specific heat of water( $\text{kJkg}^{-1}\text{C}^{-1}$ ),  $h_3$  is the enthalpy in state point 3 ( $\text{kJkg}^{-1}$ ),  $h_4$  is the enthalpy in state point 4( $\text{kJkg}^{-1}$ ), and  $t_8, t_9$  are the inlet and outlet water temperature of the condenser in Fig. 3. respectively.

Heating capacity  $Q_c$ :

$$Q_c = q_{mf} (h_3 - h_5) \quad (3)$$

Where,  $h_5$  is the enthalpy in state point 5( $\text{kJkg}^{-1}$ ).

Heating  $COP$ :

$$COP = \frac{Q_c}{P} \quad (4)$$

Where,  $Q_c$  is heating capacity( $\text{kW}$ ),  $P$  is power input( $\text{kW}$ ).

From equation (2)-(3) we can see that,

$$\begin{aligned} COP &= \frac{Q_c}{P} = \frac{q_{mf} (h_3 - h_5)}{P} = \frac{cm(t_9 - t_8)(h_3 - h_5)}{P(h_3 - h_4)} \\ &= f(c, m, t_8, t_9, h_3, h_4, h_5, P) \end{aligned} \quad (5)$$

1) First, calculate the uncertainty of each parameter,  $u_c, u_m, u_{t8}, u_{t9}, u_{h3}, u_{h4}, u_{h5}, u_P$ .

2) Second, calculate the combined standard uncertainty

$$u_{COP} = \sqrt{\left(\frac{\partial f}{\partial c} \cdot u_c\right)^2 + \left(\frac{\partial f}{\partial m} \cdot u_m\right)^2 + \left(\frac{\partial f}{\partial t_8} \cdot u_{t8}\right)^2 + \left(\frac{\partial f}{\partial t_9} \cdot u_{t9}\right)^2 + \left(\frac{\partial f}{\partial h_3} \cdot u_{h3}\right)^2 + \left(\frac{\partial f}{\partial h_4} \cdot u_{h4}\right)^2 + \left(\frac{\partial f}{\partial h_5} \cdot u_{h5}\right)^2 + \left(\frac{\partial f}{\partial P} \cdot u_P\right)^2} \quad (6)$$

3) Third, calculate the related expanded uncertainties (expanded factor=2).

$$U_{rel} = \frac{u_{COP}}{COP} \quad (7)$$

Tab.1.shows the specifications of the compressor; the specifications and uncertainties of each sensor for measuring data was shown in Tab.2. When the prototype was steadily running more than 1 hour under the selected operating mode, the all measured data were recorded only if their fluctuation was within 2 %.

**Tab.1. Specific performance of compressor (for experiment)**

Normal Power Input/HP	Vapor Discharge Mass/m <sup>3</sup> h <sup>-1</sup>	ARI Working Condition		Weight/kg	High/mm
		7.2/54.4 °C			
		Cooling Capacity/W	Power Input/W		
5	8.61	8900	2680	28	406

Notes: ARI, American Air-Conditioning and Refrigeration Institute.

**Tab.2. Uncertainties of experimental parameters**

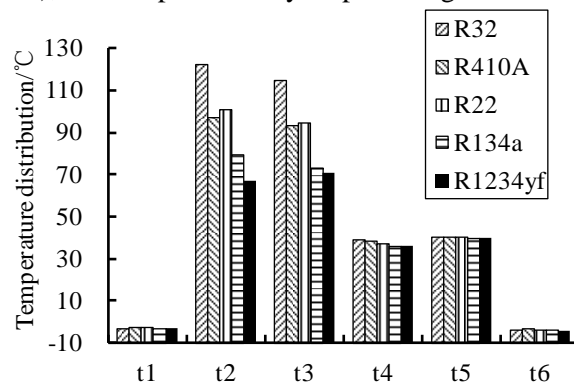
Sensor	Accuracy	Full scale	Model
Temperature	±0.15 °C	-	Pt100
Pressure transducer	±0.5% of full scale	4.5MPa	Huba
Flow meter	±0.2% of full scale	10 m <sup>3</sup> /h	LZB-50
Power acquisition unit	±0.5% of full scale	10kW	DZFC-1
Data logger	±0.2% of full scale	-	HP34972A
Heating capacity	2.1%		
Heating COP	3.4%		

The test conditions were condensing temperatures,  $t_k$ , of 45 °C and a suction superheat of 1-10 °C, a degree of liquid sub cooling of 5 °C. The evaporating temperature to was set  $t_o$  -20-0 °C.

### 3. Results and Discussions

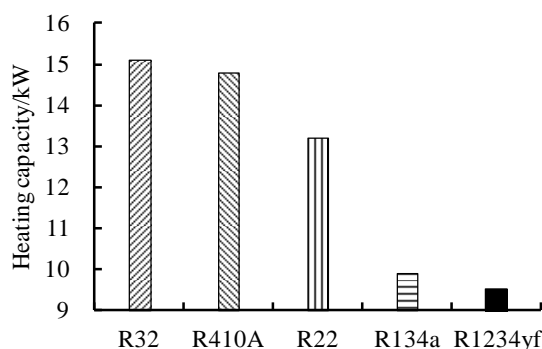
#### 3.1. Comparison of different refrigerants

The comparison of different refrigerant, including R32, R410A, R22, R134a and R1234yf of the SS system are shown in Fig.5-7, under the condition of evaporating temperature was set to -10 °C and condensing temperature was set to 45 °C. For all the five refrigerants, the overall variations of the temperature are very similar, R1234yf owns the lowest temperature. For example, the discharge pressure,  $t_2$  was about 67 °C and the highest of R32 were 118 °C, respectively. If the discharge temperature continues to increase (the evaporating temperature is lower than -10 °C or the vapor suction temperature increases), the compressor may stop running.



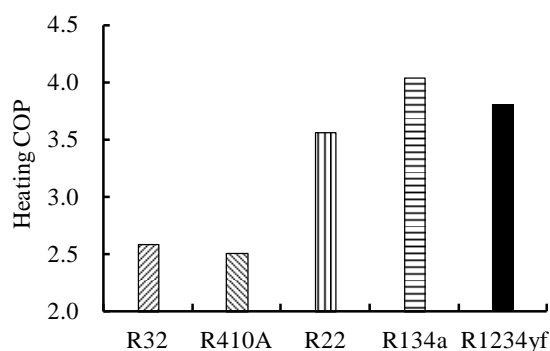
**Fig. 5. Comparison of temperature distribution for different refrigerant**

Fig.6. and Fig.7. show the heating capacity and heat *COP* with the above five kinds of refrigerants using the same compressor. From Fig.6. we can see that R32 and R410A own the highest heating capacity value among the five refrigerants while R1234yf owns the lowest. The R1234yf was lower by 28% and 3.9% relative to those of the R22 system and R134a system.



**Fig. 6. Comparison of heating capacity for different refrigerant using the same compressor ( $t_o=-10\text{ }^\circ\text{C}$ )**

From Fig.7. we can see that, R134a owns the highest heating *COP* value, it can reach up to 4.04 while R32 and R410A only own 2.5, and R1234yf was 5.9% lower than R134a. The reason is that on one hand, the R1234yf has the smallest condensation latent heat under the same vapor suction volume; one the other hand, the discharge refrigerant enthalpy for compression R1234yf is even less, so R1234yf gets the highest heating *COP* among the other refrigerants.



**Fig. 7. Comparison of heating *COP* for different refrigerant using the same compressor ( $t_o=-10\text{ }^\circ\text{C}$ )**

### 3.2. Effect of vapor suction superheat

For the R1234yf system, in order to analyze the influence of the vapor suction superheat on the compressor's performance, two tests were performed at the conditions ( $t_o=-20\text{ }^\circ\text{C}$  and  $-10\text{ }^\circ\text{C}$ ,  $t_k=45\text{ }^\circ\text{C}$ ). In these tests, the vapor suction superheat from  $1\text{ }^\circ\text{C}$  to  $13\text{ }^\circ\text{C}$ . The results are presented on Fig.8. From Fig.8. we can see that the discharge temperature increases with the rise of  $t_s$ , but it is not higher than  $95\text{ }^\circ\text{C}$  even under the evaporating temperature of  $-20\text{ }^\circ\text{C}$ .

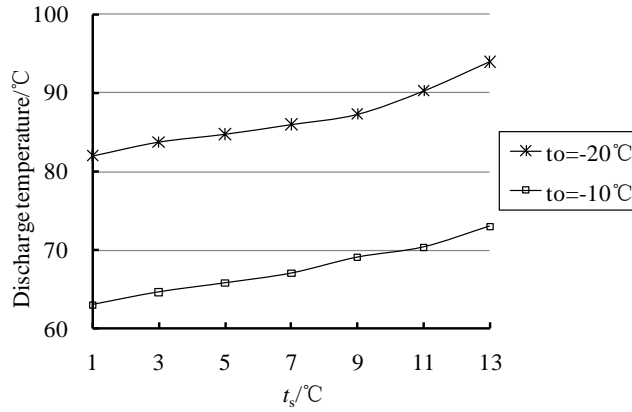


**Fig. 8. The variation of discharge temperature with  $t_s$**

The variations of the heating performance, including power input, heating capacity and heating *COP* with vapor suction superheat,  $t_s$ , are shown in Fig.9.

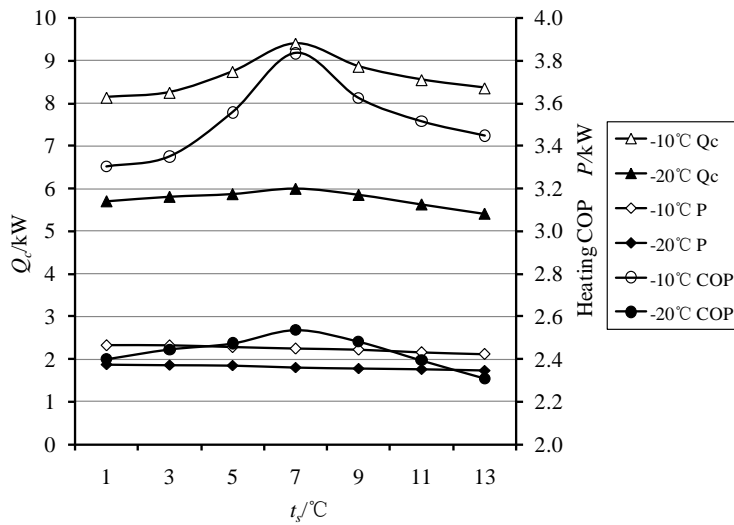


**Fig.9. The variation of heating performance with  $t_s$**

As shown in Fig.9, the power input decreases with the rise of  $t_s$ , but the decrease ratio is very little. For example, under the evaporating temperature is  $-20^\circ\text{C}$ , when  $t_s$  is  $1^\circ\text{C}$ , the power input is  $2.37\text{kW}$ , and when  $t_s$  increases to  $13^\circ\text{C}$ , the power input decreases to  $2.34\text{kW}$ , so the decrease ratio is only  $1.26\%$ . The heating capacity increases firstly, and then decreases with the increase of  $t_s$ , and heating capacity obtains the highest value. The reason is that with the increase of  $t_s$ , on one hand, it leads to the increase of the discharge temperature degree (also, it can be seen as the increase of the inlet enthalpy of the condenser); on the other hand, the increase of  $t_s$  leads to the decrease of vapor discharge mass out of the compressor, and this leads to the decrease of the condenser's heating capacity. The tendencies of the impact of the two factors on the heating character are different; the combined impact leads to a heating *COP* increase firstly, and then a decrease with the rise of the  $t_s$ . If aiming at the highest heating *COP*, the favourable value of  $t_s$  should be about  $7^\circ\text{C}$ . These results are fundamental for designing and operating the R1234yf system with vapour injection.

In prior studies, the power input was observed to decrease very little as the  $t_s$  was increased from  $1^\circ\text{C}$  to  $13^\circ\text{C}$ . When  $t_s$  is about  $7^\circ\text{C}$ , the heating *COP* also obtains the highest value. For example, under the evaporating temperature is  $-10^\circ\text{C}$ , the highest value of the heating *COP* is  $3.83$ , and under the evaporating temperature is  $-20^\circ\text{C}$ , heating *COP* can reach to  $2.54$ .



### 3.3. Effect of vapor injection

Fig.10. shows the heating performance comparison of R1234yf vapor injection system (VI system) and single stage compression system (SS system). From Fig.10. we can see that for evaporating temperature from  $-20^{\circ}\text{C}$  to  $-10^{\circ}\text{C}$ , the power input  $P$  was 4-17% higher than that of the single-stage system, respectively. Switching from a single-stage to vapor injection mode, there was a 6.2-14.3% increase in the capacity of the system, which is a big advantage in meeting the required heating demand. As shown in Fig.10. Compared with the single system, the heating  $COP$  can increase in range from 4.8 % to 11.7%.

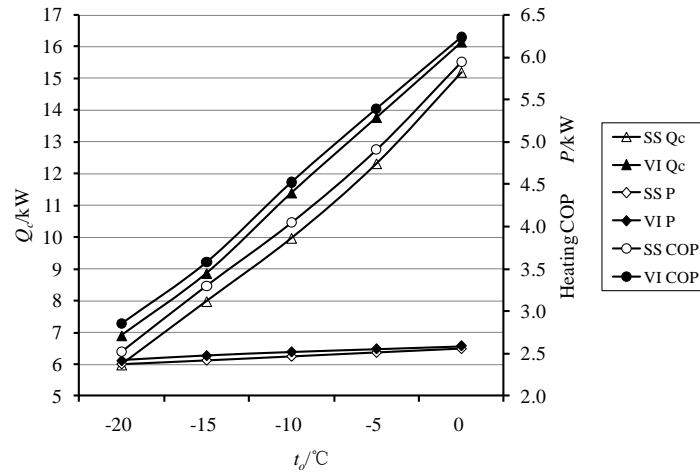


Fig. 10. Comparison of heating performance with  $t_e$

### 4. Conclusions

In this research, an R1234yf heat pump at low ambient temperature was designed, constructed and tested, and it was also compared with other commonly used refrigerants. Based on the experimental results, the following conclusions were drawn:

1) Compared with other commonly used refrigerants, the R1234yf system presents the lowest heating capacity and lowest discharge temperature when using the same compressor under the same conditions; the discharge temperature of R1234yf can be significantly lower, by  $10\text{--}20^{\circ}\text{C}$ ; and the system can run safely for a long time even under an evaporating temperature of  $-20^{\circ}\text{C}$ .

2) Running under the same conditions, the heating capacity of R1234yf is 28% and 3.9% lower than the R22 and R134a systems; for heating  $COP$ , R1234yf is 5.9% lower than R134a.

3) Discharge temperature is always increasing in R1234yf, since the vapor suction superheat increases, but it does not go higher than  $95^{\circ}\text{C}$ , even when the vapor suction superheat increases to  $13^{\circ}\text{C}$  under an evaporating temperature of  $-20^{\circ}\text{C}$ . Vapor suction superheat also influences the heating capacity and heating  $COP$ ; in this study, the optimal vapor suction superheat parameter is  $t_s = 7^{\circ}\text{C}$ .

4) Compared with a single-stage R1234yf system, the heating capacity is 14.3% higher and the heating  $COP$  is 11.7% higher for a vapor injection R1234yf system.

### Acknowledgements

This research was financially by the General project of science and technology program of Beijing Education Committee (Grant No. SQKM201810005011), Yong Top-Notch Talents Team Program of Beijing

Excellent Talents Funding(2017000026833TD02) and Hebei provincial science and technology projects in 2017 (17274515).

## Nomenclature

$c$	specific heat of water ( $\text{kJkg}^{-1}\text{C}^{-1}$ )
$h$	enthalpy ( $\text{kJkg}^{-1}$ )
$m$	mass flow rate of water ( $\text{kgs}^{-1}$ )
$k$	factor of vapor injection pressure
$P$	power input (kW)
$p_c$	condensing pressure (MPa)
$p_e$	evaporating pressure (MPa)
$p_m$	vapor injection pressure (MPa)
$q_{mf}$	refrigerant mass flow rate ( $\text{kgs}^{-1}$ )
$Q_c$	heating capacity (kW)
$t$	temperature ( $^{\circ}\text{C}$ )
$t_k$	condensing temperature ( $^{\circ}\text{C}$ )
$t_o$	evaporating temperature ( $^{\circ}\text{C}$ )
$t_s$	vapor suction temperature ( $^{\circ}\text{C}$ )
$u$	uncertainty
VI	Vapor Injection System
SS	Single Stage Compression System
$COP$	Coefficient of Performance
$GWP$	Global Warming Potential
$ODP$	Ozone Depletion Potential

## References

- [1]Peng,Q.H.,Du.Q.G.,Progress in heat pump air conditioning systems for electric vehicles—a review, *Energies*, 9 (2016),4,pp.1-17.
- [2]Chang,S.Y.,Kim,S.M.,*et al.*,Performance and heat transfer characteristics of hydrocarbon refrigerants in a heat pump system, *Int. J. Refrig*, 23 (2000),3, pp. 232-242.
- [3] Zhao,Y., Wu, X., Retrofits and options for the alternatives to HCFC-22, *Energy*, 59(2013), pp.1-21.
- [4]Patil, M.S., Kim,S.C.,*et al.*,Review of the thermo-physical properties and performance characteristics of a refrigeration system using refrigerant-based nanofluids,*Energies*,9(2016),1, pp.1-16.
- [5]Yang,M.H., Wang,B.L., *et al.*, Evaluation of two-phase suction, liquid injection and two-phase injection for decreasing the discharge temperature of the R32 scroll compressor, *Int. J. Refrig*, 59(2015), pp.269-280.
- [6]Mota-Babiloni,A., Navarro-Esbri, J., *et al.*,Drop-in energy performance evaluation of R1234yf and R1234ze(E) in a vapor compression system as R134a replacements, *Applied Thermal Engineering*,71(2014),1, pp. 259-265.
- [7]Bolaji,O., Huan, Z., Performance Investigation of Some Hydro-Fluorocarbon Refrigerants with Low Global Warming as Substitutes to R134a in Refrigeration Systems, *Journal of Engineering Thermophysics*,23(2014),2, pp.148-157.

- [8]Zilio, C., Brown, J.S., *et al.*, The refrigerant R1234yf in air conditioning systems. *Energy*, 36(2011),10, pp.6110-6120.
- [9]Navarro-Esbri,J., Moles,F., *et al.*, Experimental analysis of the internal heat exchanger influence on a vapor compression system performance working with R1234yf as a drop-in replacement for R134a,*Applied Thermal Engineering*, 59(2013),1-2,pp.153-161.
- [10]Xu,S.X., Fan, X.S., *et al.*, Experimental investigation on heating performance of gas-injected scroll compressor using R32, R1234yf and their 20wt%/80wt% mixture under low ambient temperature, *Int. J. Refrig*,75(2017), pp.286-292.
- [11]Dutta, A.K., Yanagisawa, T., *et al.*, A study on compression characteristic of wet vapor refrigerant, *Proceedings*,International Compressor Engineering Conference, Purdue University, USA, 1996,PP.235-240.
- [12]Dutta, A., Yanagisawa, T., *et al.*, An investigation of the performance of a scroll compressor under liquid refrigerant injection,*Int. J. Refrig*, 24(2001),6, PP. 577-587.
- [13]Winandy,E., Lebrun, J., Scroll compressors using gas and liquid injection: experimental analysis and modeling, *Int. J. Refrig*, 25(2002),8, PP.1143-1156.
- [14]Cho, H. T., Chung, J., *et al.*, Influence of liquid refrigerant injection on the performance of an inverter-driven scroll compressor, *Int. J. Refrig*,26(2003),1, PP. 87-94.
- [15]Navarro, E., Redon, A., *et al.*, Characterization of a vapor injection scroll compressor as a function of low, intermediate and high pressures and temperature conditions, *Int. J. Refrig*,36(2013),7,PP. 1821-1829.
- [16]Zhang, Z.Q., Li, W.Y., *et al.*, A study on electric vehicle heat pump systems in cold climates. *Energies*, 9(2016), 12, PP. 1-11.
- [17]Bell, I., Groll, E., *et al.*, Simulation of a cold climate heat pump furnished with a scroll compressor with multiple injection lines, *Proceedings*, the 8th International Conference on Compressors and their Systems, City University London,UK, 2013, PP.87-101.
- [18]Guo, W., Ji, G.F., *et al.*, R32 compressor for air conditioning and refrigeration applications in China, *Proceedings*, International Compressor Engineering Conference, Purdue University, USA, 2012,PP.1-8.
- [19]Xu, S. X., Ma, G.Y., *et al.*, Experiment study of an enhanced vapor injection refrigeration/heat pump system using R32. *International Journal of Thermal Science*, 68(2013), 2, PP.103-109.
- [20]Xu, X., Hwang, Y., *et al.*, Performance comparison of R410A and R32 in vapor injection cycles. *Int. J. Refrig*, 36(2013), 3, PP.892-903.
- [21]Xu, X., Hwang, Y., Radermacher R. Refrigerant injection for heat pumping/air conditioning systems: literature review and challenges discussions. *Int. J. Refrig*, 34(2011),2, PP.402-415.

Paper submitted: 19.10.2017.

Paper revised: 07.06.2018.

Paper accepted: 07.07.2018.